

CFD STUDY OF SHOCK CONTROL AT CRANFIELD

N Qin, Y Zhu and PR Ashill
Centre for Computational Aerodynamics
Cranfield University College of Aeronautics
Bedford MK43 0AL, England, UK
n.qin@cranfield.ac.uk

Keywords: *shock control, transonic, CFD, aerodynamic performance*

Abstract

This paper presents some recent research results at Cranfield on parametric studies of various shock controls at transonic speeds using Navier-Stokes solutions. The effects of suction, blowing and solid bumps on aerofoil aerodynamic performance have been studied systematically regarding the control location, the mass flow strength and the bump height. Comparisons with experimental data have been made where possible to validate the numerical study. The numerical simulation highlighted the benefits and drawbacks of various types of control for transonic aerodynamic performance and identified some key parameters.

1 Introduction

Modern commercial transport aircraft relies on cruising very near to the initial drag rise condition, i.e. the drag-rise Mach number. The condition penetrates into the transonic region, in order to achieve the high speed and the near maximum value of the parameter $M_{\infty}C_L/C_D$ that are required for maximum payload, range and operating economy. Therefore, weak shocks will probably already have formed on the wing at the cruise conditions. An increase in either Mach number or incidence will cause the shock wave to move back along the aerofoil surface until its progressively increasing pressure rise becomes too large for the boundary layer to negotiate without separating [1].

The interaction between a shock wave and a boundary layer often leads to extremely detrimental effects, especially if the shock is strong enough to separate the boundary layer.

When this happens, there occurs a rapid growth of the boundary layer along with a dramatic increase in large-scale fluctuation leading to the occurrence of buffeting. The appearance of strong shock waves on aircraft wings at high subsonic speed also marks the onset of a rapid rise in the drag. This drag rise has the effect of limiting the performance of the aircraft by inhibiting speed, range and manoeuvrability. Delaying the drag-rise through flow control can extend the operational speed, reduce aircraft drag and the delay the buffet onset.

Recently, a number of control methods have been proposed for improving the aerodynamic performance through either weakening the shock wave or energising the boundary layer [2-10]. The aim of the present work is to investigate key parameters in shock control methods, including blowing, suction, and the use of surface bumps, on aerofoil aerodynamic performance, represented by the lift-drag ratio, using an effective Computational Fluid Dynamics (CFD) method.

2 Physical Model and Solution Method

2.1 Governing equations

The governing equations are the Favre-averaged Navier-Stokes equations in their integral form. An algebraic turbulence model is employed for the closure of the Reynolds stress terms arising from the averaging process. The basic formulation follows that proposed by Baldwin and Lomax [11]. For the flow problems studied in the present paper, the effect of mass transfer at the wall is modelled by using the corrected van Driest factor proposed by Cebeci [12]

$$A^+ = 26 \left\{ -\frac{p^+}{v_w^+} [\exp(11.8v_w^+) - 1] + \exp(11.8v_w^+) \right\}^{-1/2} \quad (1)$$

where

$$p^+ = -\frac{(dp/d\xi)_w \mu_w}{\rho_w^2 (u_w^*)^3} \quad (2)$$

$$v_w^+ = \frac{v_w}{u_w^*} \quad (3)$$

and $(dp/d\xi)_w$ is the pressure gradient at the wall in the streamwise direction, μ_w is the molecular viscosity at the wall, and u_w^* is the friction velocity given by

$$u_w^* = \left(\frac{|\tau_w|}{\rho_w} \right)^{1/2} \quad (4)$$

where ρ_w and τ_w are the density and the shear stress at the wall respectively.

2.2 Methodology

The flow governing equations are solved using the finite-volume approach, where the conservation laws are enforced on each computational cell (finite-volume). The variation of the conserved properties with time in a given cell is balanced by the fluxes through the cell's boundary. In the present method, an approximate Riemann solver, the Osher scheme [13], is used for the convective flux calculation at the cell interfaces. The local Riemann problems are solved with the left and right states "reconstructed" by the MUSCL scheme. A slope limiter is employed to prevent oscillations at the shock wave.

In the numerical studies, the solution sensitivity to the grid was investigated to determine a reasonable grid for the numerical testing on flow controls. Grid adaptation [14] based on the equidistribution principle, has been used to address the grid sensitivity issue in an

efficient way. Further details of the numerical method can be found in [15].

2.3 Boundary conditions

At the far field boundaries, the characteristic boundary conditions are applied. In the present study of two-dimensional flows over aerofoils, this implies either subsonic inflow or subsonic outflow boundary conditions. At the solid wall on the aerofoil, the no-slip boundary condition is specified. At the surface with mass transfer, the normal velocity component is determined by

$$v_w = \frac{C_Q \rho_\infty U_\infty c}{\sum_{L_{suction}} \rho_w \Delta s}, \quad (5)$$

where the suction/blowing coefficient is defined as

$$C_Q = \frac{\dot{m}}{\rho_\infty U_\infty c} = \frac{1}{\rho_\infty U_\infty c} \int_{s_1}^{s_2} \rho_w v_w ds. \quad (6)$$

For the relatively weak suction and blowing considered in this study, the viscous boundary conditions can reasonably be applied. In addition to the above normal velocity component, the tangential velocity component is determined from the suction/blowing inclination angle.

2.4 Force calculation and system consideration

In the case of suction, mass is removed from the flow external to the aerofoil surface. Obviously, the same amount of mass has to be ejected somewhere from the aerofoil into the main flow to conserve mass. From the conservation of momentum, or Newton's second law, there will be a force acting on the aerofoil in addition to the pressure and skin-friction forces acting on the external surfaces of the aerofoil. However, this force will depend on how the sucked air is ejected into the main flow. These include factors such as where to eject, at what direction and at what speed. The ejection itself in turn will also influence the flowfield and, therefore, pressure and skin friction forces on the aerofoil. Furthermore, for practical application, it is

necessary also consider cost for the installation of the pipeline system inside the aircraft, the power required to run the pump and the losses in the pipe system. This highlights the importance of considering the system as a whole for successful implementation of flows control devices involving mass flows.

The current study is limited to the study of the effect of suction control on the flowfield as an isolated factor. Therefore, the above-mentioned system integration issues are not discussed further in this paper, although they would obviously have to be investigated in a more general study. It is assumed that the air sucked from the mainstream is ejected out through a pipeline normal to the aerofoil cross section at the pipe exit. Therefore there is no contribution to the lift and drag forces from the ejected air. This also what has been done in some experimental studies on suction aerofoils, which are used to assess the present methodology, e.g. [8].

Similarly, for the cases of blowing, the present studies are limited only to isolated effects of blowing on the forces acting on the aerofoil.

3 Validation

3.1 NACA64A010 Aerofoil with suction

The NACA64A010 aerofoil was tested extensively by Smith and Walker [16] at transonic conditions with a surface suction downstream of the hinge line of the trailing-edge flap. The flow conditions investigated in the experiment were at a Reynolds number of 2.9 million based on aerofoil chord for a range of Mach numbers from 0.70 to 0.84 and a range of angles of incidence from -1° to 4° . Both the suction parameter and the flap angle were varied in the experiments.

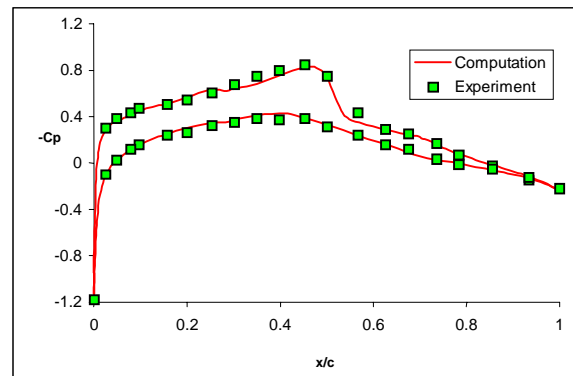


Figure 1. Surface pressure distribution around NACA64A010 aerofoil without suction

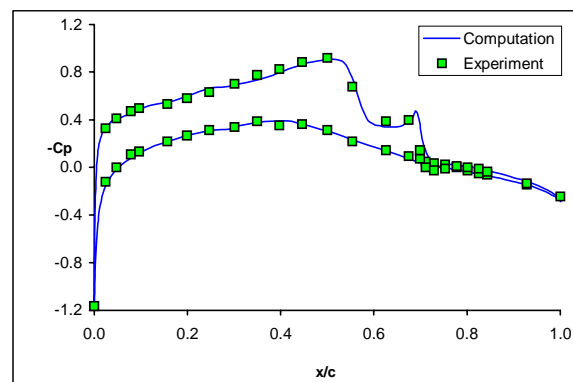


Figure 2. Surface pressure distribution around NACA64A010 aerofoil with suction

The flow conditions chosen for computation were $M_\infty=0.78$, $\alpha=0.5^\circ$ and $Re=2.9 \times 10^6$ corresponding to one of the wind tunnel experimental conditions. In the experiment, the suction region was located between 69% to 72.5% of chord length from the leading edge, which is downstream of the shock position without suction. The suction coefficient was 0.00225, with a trailing edge flap deflection of 1° . The suction angle β was chosen to be 84° to the aerofoil surface since the suction is normal to the chord line. The flow was assumed to be fully turbulent.

For quantitative comparison, the pressure distributions from both the computation and the experiment, with and without suction, are compared in Figs.1 and 2 respectively. These figures show that the computation is in good agreement with the experimental data in both cases. The effect of the surface suction is captured quite well.

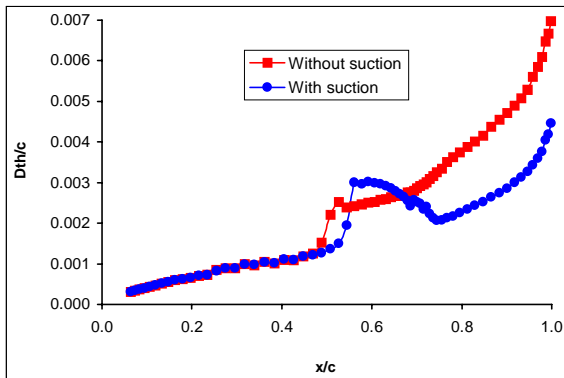


Figure 3. Computed boundary-layer displacement thickness on NACA64A010 aerofoil.

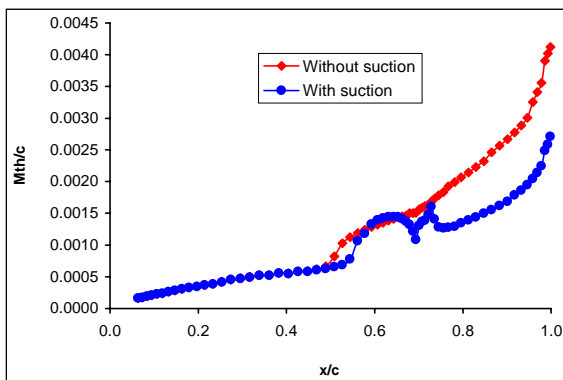


Figure 4. Computed boundary-layer momentum thickness on NACA64A010 aerofoil.

Figure 3 shows the predicted boundary-layer displacement thickness, δ^* , both with and without suction. It shows that the displacement thickness has a sudden increase under the shock wave. Upstream of the shock, suction has little effect on the displacement thickness, except that the shock is displaced slightly downstream. Immediately downstream of the shock the displacement thickness is increased by the suction, but only after a small distance further downstream this soon drops down below the corresponding ‘no-suction’ value on the last third of the aerofoil downstream of the suction region. Figure 4 shows the computed momentum thickness θ both with and without suction. The effect of suction is similar to that on the displacement thickness.

The skin-friction distributions on the upper surface of the aerofoil are plotted in Figs.5 and 6 for the cases with and without suction. Very high skin-friction over the suction region

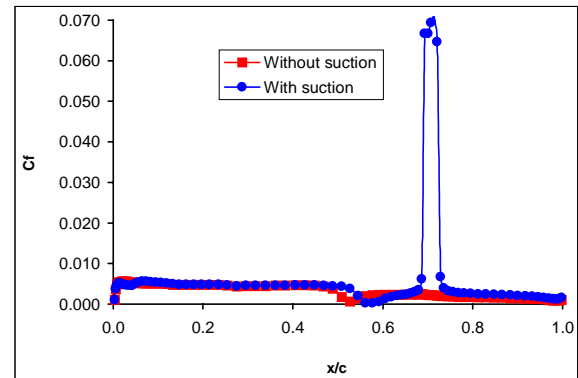


Figure 5. Computed skin-friction distributions on NACA64A010 aerofoil – overall picture

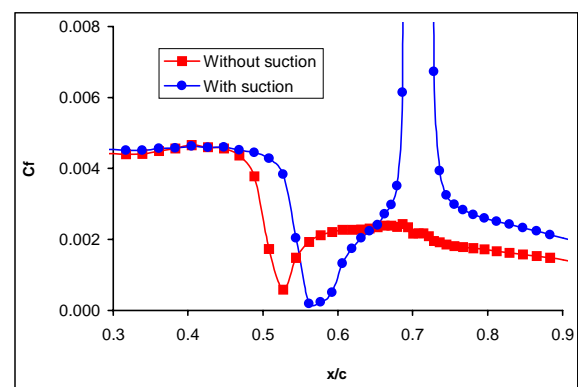


Figure 6. Computed skin-friction distributions on NACA64A010 aerofoil – local behaviour

can clearly be observed, contributing to the skin friction drag. For both cases, the skin friction reduces to a value near zero locally (Fig.6) due to the effect of the strong adverse pressure distribution created by the shock wave. Since suction actually strengthens the shock in this case, the skin-friction becomes closer to the incipient separation condition with suction. This indicates that suction downstream can promote shock-induced separation locally (bubble type).

For this downstream suction case, both lift and drag are increased by the effect of suction. However the lift increase is more substantial, resulting in an increase in the L/D ratio [10].

3.2 RAE5243 Aerofoil with suction

The RAE5243 aerofoil with a maximum thickness-chord ratio of 14% is a natural laminar flow aerofoil (NLF) with a pressure distribution on the upper surface having a favourable pressure gradient upstream of the shock at about 55% chord. The aerofoil has a

very slight blunt trailing edge (0.5%*c*). The flow conditions were $M_\infty=0.6799$, $Re=18.68\times 10^6$, corresponding to the wind tunnel experiment by Fulker and Simmons [7]. The angles of incidence measured in the experiment for both cases (with and without suction) to be studied are $\alpha=0.77^\circ$. The suction region is located at 45-46% chord length from leading edge with suction coefficient $C_Q=9\times 10^{-5}$ and suction angle $\beta=89^\circ$. It is a case of weak suction about 10% chord upstream of the shock wave.

Initial studies revealed that a proper treatment of the trailing edge is crucial for the accurate prediction of aerofoil lift and drag. A multi-block solution approach has to be adopted to provide a precise simulation of the trailing edge flow although the bluntness is only 0.5% chord.

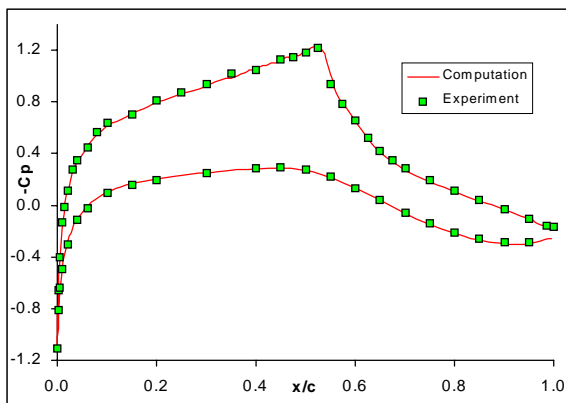


Figure 7. Surface pressure distribution around RAE5243 aerofoil without suction

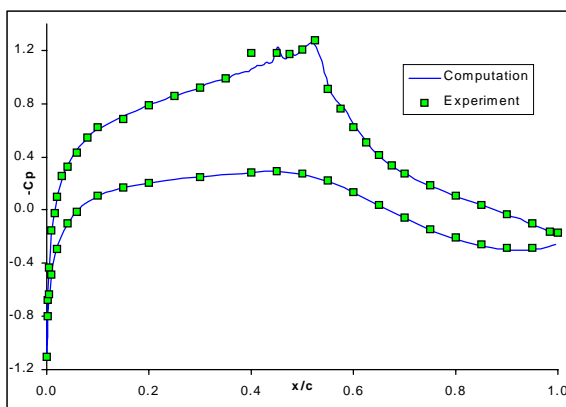


Figure 8. Surface pressure distribution around RAE5243 aerofoil with suction

Figs. 7 and 8 show the computational and experimental pressure distributions for the

RAE5243 aerofoil for cases without and with suction, respectively, at the same experimental normal force coefficient. The figures show that the computation is in excellent agreement with the experimental data for both cases. Note that the trailing edge pressure is slightly open due to the slight bluntness of the trailing edge.

3.3 RAE5225 Aerofoil with surface bump

The RAE5225 aerofoil is a supercritical aerofoil with a maximum thickness to chord ratio of 14%. The flow condition chosen for the computational test were $M_\infty=0.73$ and $Re=6.1\times 10^6$ with transition fixed at 5% chord on both upper and lower surfaces corresponding to the wind tunnel experiment by Fulker, *et al.* [6]. A bump was fixed at 40~60% chord position on the upper surface.

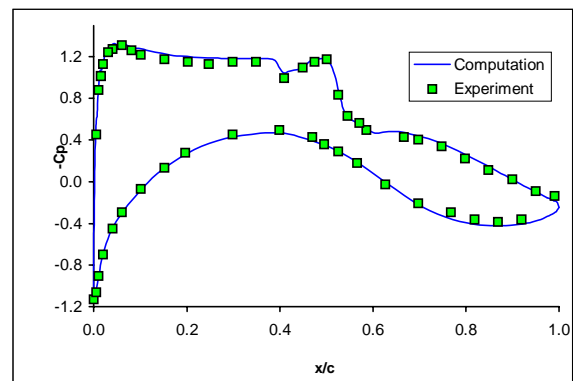


Figure 9. Surface pressure distribution around RAE5225 aerofoil with surface bump

Figure 9 shows the computational and the experimental pressure distributions for the RAE5225 aerofoil with 0.175% chord length height bump at 40~60% chord length from the leading edge. It shows that the computation is in good agreement with the measurement.

4 Parametric Studies of Effects on Aerodynamic Performance

4.1 Suction

The effect of the position of suction regions relative to the shock position is illustrated in Figs. 10 and 11 for the RAE5225 aerofoil case, where $M_\infty=0.734$, $\alpha=3^\circ$ (for Fig.10 only), $C_Q=5\times 10^{-4}$. Clearly, suction changes the local

pressure significantly. The aerofoil performance can be improved by suction located at or downstream of the shock position. On the other hand, when the suction position is upstream of the shock position, the aerodynamic performance is degraded (Figure 11).

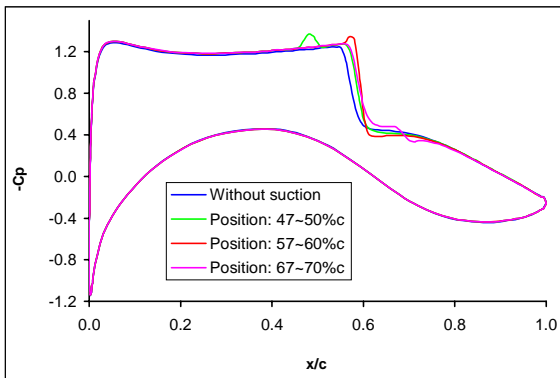


Figure 10. Surface pressure distribution around RAE5225 aerofoil – effect of suction position

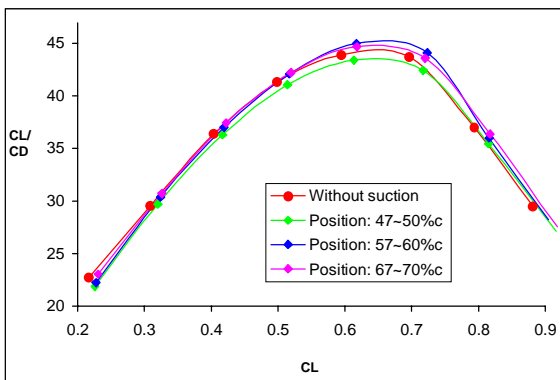


Figure 11. Lift-drag ratio for RAE5225 aerofoil – effect of suction position

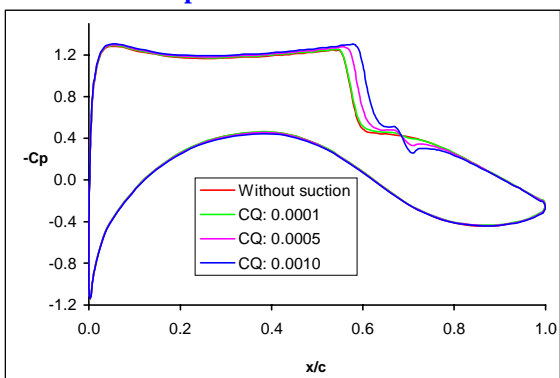


Figure 12. Surface pressure distribution around RAE5225 aerofoil – effect of suction mass flow

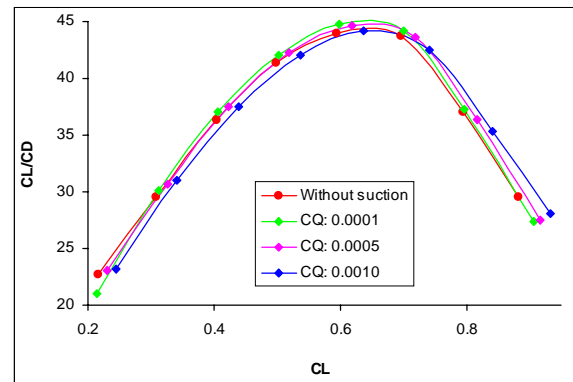


Figure 13. Lift-drag ratio for RAE5225 aerofoil – effect of suction mass flow

The suction strength also has a strong effect on the aerofoil surface pressure distribution and the L/D ratio. Figs.12 & 13 show the results for $M_\infty=0.734$, $\alpha=3^\circ$ (for Fig.12 only) and suction position at 67-70% c. Increasingly stronger suction has an effect of pulling the shock downstream (Figure 12) and shifting the L/D ratio curve to the right in the higher lift region (Figure 13). This indicates that while stronger suction can improve the performance in the high lift region the performance in the low lift region can be degraded.

It was also revealed that the near tangential suction is more beneficial than near normal suction, giving a high lift-drag ratio.

4.2 Bump

Figure 14 shows the RAE5243 aerofoil datum section with 0.175% chord high bump at 40~60% chord. The flow conditions are $M_\infty=0.68$, $Re=19 \times 10^6$ with transition fixed at 5% chord on both upper and lower surfaces.

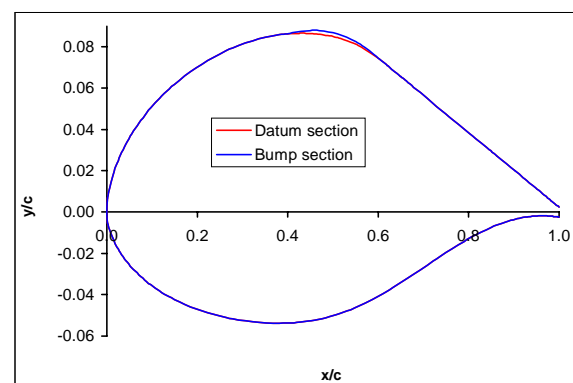


Figure 14. RAE5243 aerofoil with bump

Figs. 15&16 show the pressure distributions for the RAE5243 aerofoil at an angle of incidence $\alpha=2.5^\circ$ for three bump positions. The figure demonstrates the sensitivity of the pressure distribution to the bump location. When placed with its crest close to the shock the bump can serve the purpose of reducing shock strength and hence wave drag.

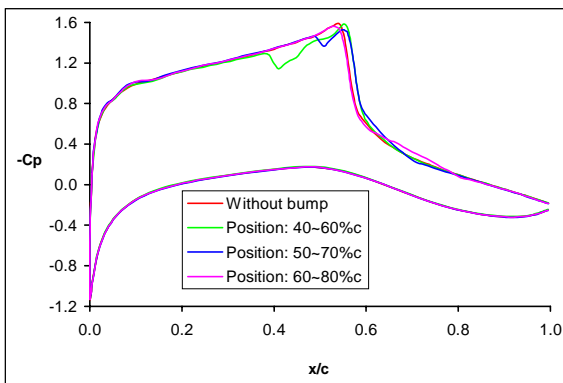


Figure 15. Surface pressure distribution around RAE5243 aerofoil – effect of bump position.

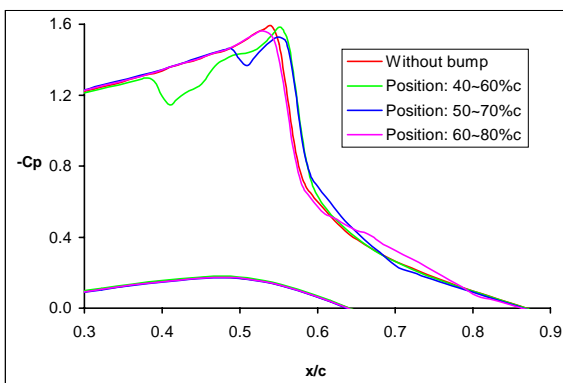


Figure 16. Surface pressure distribution around RAE5243 aerofoil – local behaviour.

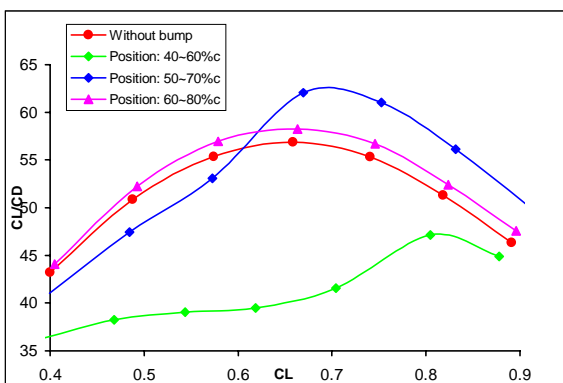


Figure 17. Lift-drag ratio for RAE5243 aerofoil – effect of bump position

It is particularly interesting to examine the effect of bump positions on L/D for a wide range of lift coefficients, as shown in Figure 17. This figure shows that a bump at 40~60% chord (ahead of the shock) reduces the L/D ratio for the whole lift range considered, while a bump at 60~80% chord (downstream the shock) increases the lift-drag ratio moderately over the same lift range. A bump at 50~70% chord (under the shock) increases the lift-to-drag ratio significantly for the high lift region but degrades the performance of the original aerofoil at the lower lift region (0.4~0.6). There is an interesting crossover at $C_L=0.6$. Note that for this NLF aerofoil the shock position is almost fixed at 55% for the incidence (lift) range considered.

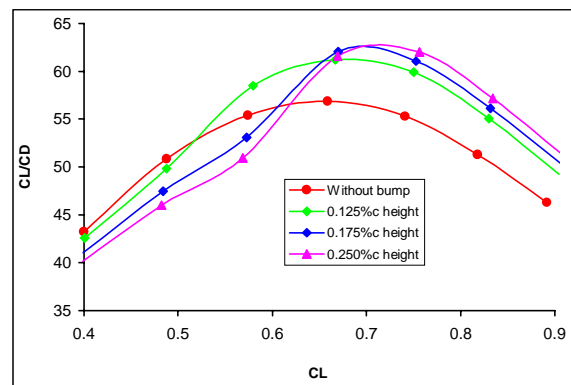


Figure 18. Lift-drag ratio for RAE5243 aerofoil – effect of bump height (position: 50-70%)

Another important parameter is the bump height as illustrated in Figure 18. This shows results for three different bump heights located at 50~70% for the RAE5243 aerofoil. It demonstrates that the higher bump gives more significant gain at higher lift range and, at the same time, more degradation at the lower lift range.

4.3 Blowing

The bump improves the aerodynamic performance by moderating the shock wave on the upper surface of the aerofoil at transonic speeds. Similar effects may also be achieved by blowing at the foot of the shock wave.

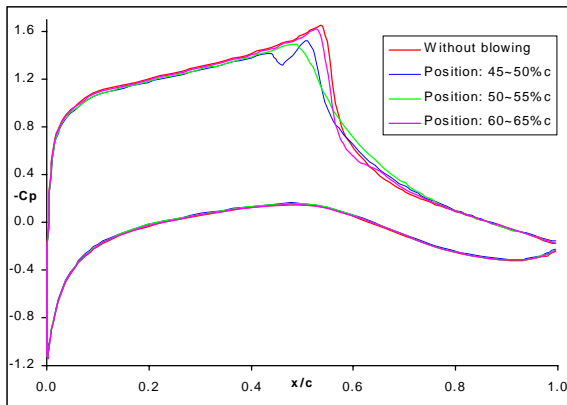


Figure 19. Surface pressure distribution around RAE5243 aerofoil – effect of blowing position

Three blowing positions, 45~50% chord, 50~55% chord, and 55~60% chord, which are classified as upstream of, under, and downstream of the shock wave respectively, were selected to investigate the effects of the blowing position. The case is for $M_\infty=0.68$, $C_Q=4\times 10^{-4}$, and the inclined blowing angle $\beta=15^\circ$.

Figure 19 shows the aerofoil pressure distributions for three blowing positions at the same incidence $\alpha=3^\circ$. It clearly shows that blowing changes the pressure distribution. The shock strength is reduced, and the shock wave moves upstream, the effect being particularly apparent when blowing is underneath the shock wave. It is interesting to see that blowing downstream of the shock wave can also slightly reduce the shock strength by moving it upstream. Blowing at 50-55% under the shock (at ~55%) is the most effective in reducing the shock strength.

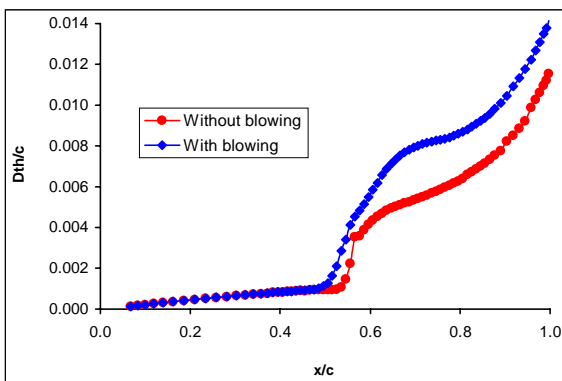


Figure 20. Computed boundary-layer displacement thickness on RAE5243 aerofoil.

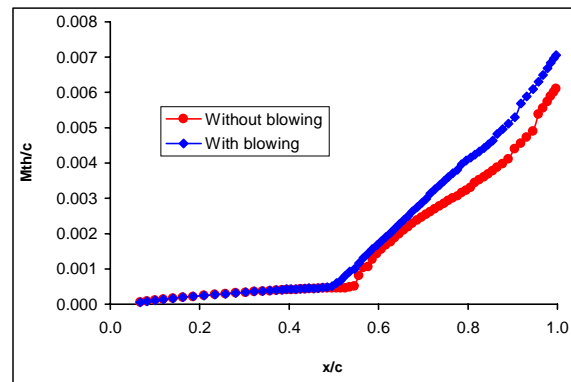


Figure 21. Computed boundary-layer momentum thickness on RAE5243 aerofoil.

Figs. 20-22 show the boundary layer behaviour and the skin friction with and without blowing. The blowing case is for the 50-55% c position. They show that blowing increases the boundary-layer thickness and reduces the skin-friction drag for a fixed incidence.

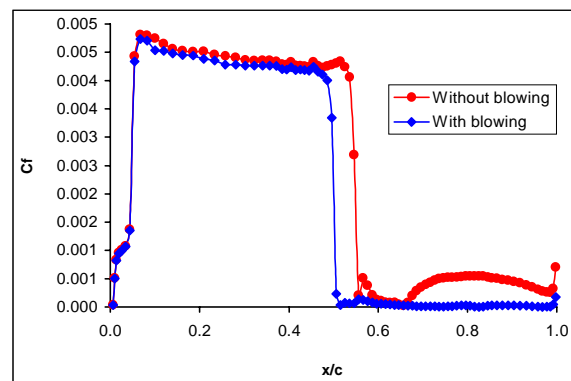


Figure 22. Computed skin-friction distributions on RAE5243 aerofoil

Figure 23 shows the lift-drag ratio plotted against lift coefficient for the blowing cases, which reveals that the blowing reduces the lift-drag ratio over the range of the lift coefficients studied.

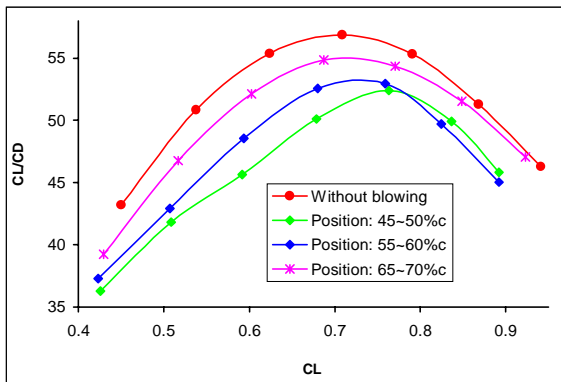


Figure 23. Lift-drag ratio for RAE5243 aerofoil – effect of blowing position

The RAE5225 aerofoil has a wider range of shock wave position as angle of incidence or Mach number changes compared with RAE5243 aerofoil. Three blowing positions were selected to investigate the effects of blowing position, at 47~50% chord, 57~60% chord, and 67~70% chord, respectively. The blowing coefficient C_Q is 5×10^{-4} , and blowing angle $\beta=45^\circ$. Again the lift-drag ratio is reduced significantly due to blowing.

Blowing further away from the shock wave has also been studied. It was found that appropriate blowing could increase the lift-drag ratio. Blowing near the trailing edge with small blowing coefficient indicated some improvement in L/D for the RAE5225 aerofoil. The blowing position in these calculations was taken to be near the trailing edge at 97.5-98% chord, with the blowing coefficients $C_Q = 0.0005$ and 0.001 and $\beta=5^\circ$.

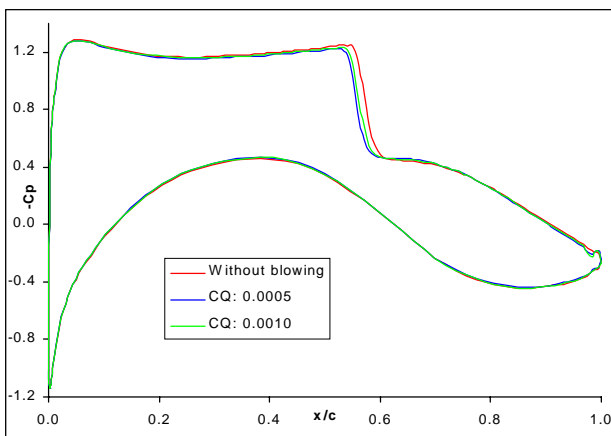


Figure 24. Pressure distribution for RAE5225 – near trailing edge blowing.

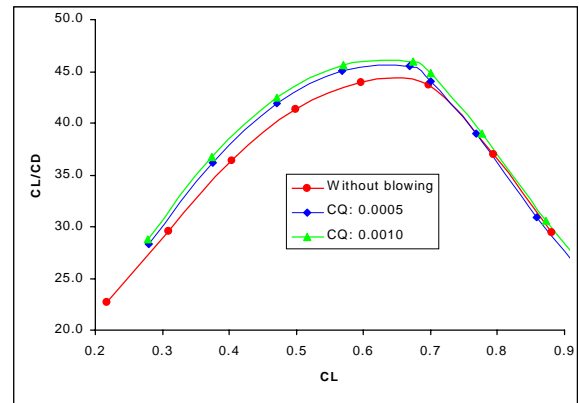


Figure 25. Lift-drag ratio for RAE5225 – near trailing edge blowing.

Figure 24 shows the pressure distributions for the RAE5225 aerofoil for $\alpha=3^\circ$ with blowing near the trailing edge. It shows that blowing far away the shock wave weakly can also weaken the shock wave, and move the shock wave upstream slightly. Figure 25 shows the lift-drag ratio against lift coefficient for the corresponding cases. It shows that weak blowing near trailing edge with a small angle to the aerofoil surface can improve the aerodynamic performance of the aerofoil for $C_L < 0.7$. It is most beneficial in the maximum lift-drag ratio region. There is very little improvement for higher lift region. Unlike the suction and bump cases, this improvement is related to the modification of the trailing edge flow (i.e. circulation) rather than the near shock behaviour.

5 Conclusion

A parametric study of shock control for transonic aerofoil flows using suction, blowing and surface bumps has been carried out. Suction and bumps can both improve the transonic aerodynamic performance. The former achieves it through significantly increased lift (stronger shock) and the latter by weakening the shock (reduced wave drag). Blowing at the shock position can significantly reduce the shock strength but with much reduced lift-drag ratio. The only situation where blowing is found to be beneficial is where it takes place near the trailing edge at a small angle (similar to the jet flap).

References

- [1] Pearcey HH. Shock-induced separation and its prevention by design and boundary layer control. In *Boundary Layer and Flow Control*, Vol. 2. Ed. G. V. Lachmann, Pergamon Press, 1961.
- [2] Stanewsky E, Delery J and Fulker J. Drag reduction through control of shock boundary layer interaction. In *Computational Methods in Applied Sciences* (Eds J.-A. Desideri et al.), 1996, pp.455-465 (John Wiley, Chichester).
- [3] Thibert JJ, Reneaux J, and Schmitt V. ONERA activities on drag reduction. ICAS 90-3.6.1, September 1990.
- [4] Ashill PR, Fulker JL, Simmons MJ and Gaudet IM. A review of research at DRA on active and passive control of shock waves. ICAS 96-2.1.4, 1996.
- [5] Ashill PR, Fulker JL and Shires A. A novel technique for controlling shock strength of laminar-flow aerofoil sections. DRA Tech Memo A&P 13, 1993.
- [6] Fulker JL, Ashill PR, and Simmons MJ. Study of simulated active control of shock waves on aerofoil sections. DRA Technical Report TR93025, 1993.
- [7] Fulker JL, Simmons MJ. An experimental study of shock control methods. DRA/AS/HWA/TR94007/1, 1994.
- [8] Fulker JL, and Simmons MJ. Drag reduction methods using active, suction, techniques-initial experimental and theoretical results. DRA/AS/HWA/CR97019/1.1, 1997.
- [9] Zhu Y, and Qin N. Control of shock induced separation by surface suction. 3rd Pacific International Conference on Aerospace Science and Technology, September 1997, Xi'an, China, pp.204~pp211.
- [10] Qin N, Zhu Y, and Poll DIA. Surface suction on aerofoil aerodynamic characteristics at transonic speeds. *Proc. Instn. Mech. Engrs Journal*, Vol. 212, Part G, pp339-351.
- [11] Baldwin B and Lomax H. Thin layer approximation and algebraic model for separated turbulent flows, AIAA paper No. 78-257, 1978.
- [12] Cebeci T. Behavior of turbulent flow near a porous wall with pressure gradient. *AIAA J*, Vol. 8, No. 12, pp 2152-2156, 1970.
- [13] Osher S and Soloman F. Upwind difference schemes for hyperbolic system of conservation laws. *Mathematics of Computation*. Vol.38, No.158, pp.339-374.
- [14] Qin N and Zhu Y. Grid Adaptation for Shock/Turbulent Boundary Layer Interaction. *AIAA J*. Vol.37, pp1129-1131, 1999.
- [15] Zhu Y. Computational study of shock control at transonic speed. PhD Thesis, College of Aeronautics, Cranfield University, March 2000.
- [16] Smith DW and Walker JH. Test of an area suction flap on a NACA64A010 airfoil at high subsonic speeds. NASA TN D310, 1960.